Novel Method for the Production of SiC micro and nanopatterns

A.S. Racz [†‖], D. Zambo [†], G. Dobrik [†], I. Lukacs[†], Z. Zolnai[†], A. Nemeth[§], P. Panjan[‡], A. Deak[†], G. Battistig[†], M. Menyhard[†]*

[†] Institute for Technical Physics and Materials Science, Centre for Energy Research, Hungarian Academy of Sciences, Konkoly Thege M. út 29-33, H-1121 Budapest, Hungary

[‖] Budapest University of Technology and Economics, Műegyetem rkp. 3, H-1111 Budapest, Hungary

[§]Wigner Research Centre for Physics, Hungarian Academy of Sciences, Konkoly-Thege M. út 29-33, H-1121 Budapest, Hungary

[‡]Jožef Stefan Institute, Jamova 39, 1000 Ljubljana, Slovenia

HIGHLIGHTS

- A novel method was demonstrated for the production of SiC micro and nanopatterns
- Patterning and SiC compound formation happened in one step at room temperature
- The SiC formation was proved by AES depth profiling
- Two different patterns were presented
- The method can be considered as a possibility to fabricate SERS substrates

ABSTRACT

In this paper we report on a novel, large area method to produce SiC nano- and micro patterns at room temperature where the compound and pattern formation happens in one step. We have previously demonstrated that SiC can be produced by noble gas irradiation of a Si/C multilayer

system utilizing the ion beam mixing (IBM) taking place at the interfaces. Here we show that by applying IBM in samples masked in any desired way patterned SiC surfaces, micro and nanostructures, result. Two different masking layers were applied to demonstrate the capabilities of the method; a Langmuir-Blodgett (LB) film of 590 nm silica nanoparticles and a lithographic grid, of 2 μm periodicity, mounted to the surface of a Si/C multilayer system. The systems were irradiated by Xe^+ ions of 120 keV. The samples before and after IBM have been analyzed by AFM, SEM and AES depth profiling, proving that patterning occurred: the non-covered areas became SiC rich regions, while the covered areas remained untouched. As a possible application for the patterned samples, the gold-coated LB patterned nanostructure was used for surface enhanced Raman spectroscopic detection of an organic dye molecule (R6G) demonstrating the efficiency of IBM for producing SERS substrates consisting of a very stable compound like SiC.

KEYWORDS: *room temperature SiC formation, ion beam mixing, nanopatterns, SERS, LB film*

1. INTRODUCTION

Silicon carbide (SiC) has drawn significant interest due to its advantageous properties such biocompatibility, high temperature strength, high modulus and inertness in corrosive environments. The application of SiC in thin film forms is also important for nano/micro-electromechanical systems (N/MEMS) in harsh environments. Although SiC thin films are mature enough to allow the fabrication of a wide variety of biochips, microelectronics and N/MEMS devices, there is still a need for a./ reducing the deposition temperatures to permit increased integration options for SiC MEMS with electronics and b./ developing suitable micro- and nanopatterning methods [1-9]. Surface nanopatterning has become more and more important due to the rapid development of nanoelectronic, photonic crystals, and biomedical devices.

Various techniques are available, such as direct laser writing, self-assembly of colloidal particles and lithography to fabricate two-dimensional (2D) and three-dimensional periodic (3D) structures [10-14]. The above methods cannot be, however, easily applied for the case of SiC [14]. Therefore novel methods are needed for fabricating patterned SiC structures.

The use of ion beams techniques is a very attractive method to control material properties. Applications of ion implantation for surface patterning increased essentially in recent decades. For example magnetic patterns were obtained by irradiating metals by several ions - N^+, P^+. He^+, Ne^+ - through a lithographically prepared or self assembled nanosphere masks [15,16]. Co and Pt ions were used to achieve nanopatterns through a nanoporous alumina mask [17]. Mesoporous silica thin films were patterned by Xe^+ through a Langmuir-Blodgett film [18].

It has been known for a long time that during ion implantation ion beam mixing (IBM) also happens [19]. During IBM compound formation may occur; as it is a non-equilibrium process it can be applied to produce compounds at room temperature for which generally high temperatures are needed. IBM has not been applied for producing patterned surfaces, however. Recently we have shown that it is possible to produce SiC nano-coating at room temperature by applying IBM on C/Si multilayer structures [20-21]; the produced coatings exhibited excellent corrosion resistance properties [22]. The simultaneous application of masks and ion irradiation on a properly chosen C/Si multilayer system would lead to one step compound and pattern formation.

In this paper we will show that the combination of masking layers with IBM allows the fabrication of patterned SiC structures at room temperature and the achievable patterned area is up scalable to wafer size. For this purpose IBM was applied on a Si/C system covered by masks

obtained by either conventional lithography technique or nanosphere lithography. Auger electron spectroscopy (AES) depth profiling showed that the produced samples exhibited nanopatterned SiC rich regions. The obtained 2D structure can be also easily transformed with simple etching and oxidation steps to a well-defined 3D structure. The 3D structure produced by applying the Langmuir-Blodgett film was tested for surface-enhanced Raman scattering (SERS) application. To our knowledge IBM have not been used to produce SERS substrates, yet. Despite the advantageous properties of SiC, only few papers have been published concerning the Raman enhancement activity of SiC-based substrates [23,24]. Kuntumalla et al. [23] have shown that silver decorated nano-ß-SiC possess SERS activity. Zhang et al. [24] fabricated SiC thin film microfluidic sensor for SERS. In our case the non-patterned SiC rich layer made by IBM and covered by gold showed Raman effect by exciting rhodamine 6G (R6G) reporter molecules. The patterning of this sample showed an enhancement of the Raman signal. In summary, our aim was twofold: firstly to demonstrate the efficiency of IBM in obtaining patterned SiC at room temperature, secondly our method could be applied for fabricating SERS substrates consisting of a very stable compound like SiC.

2. EXPERIMENTAL SECTION

2.1. Production of SiC rich layer by means of IBM

We have shown previously that IBM of layer systems containing pure C and Si layers may result in formation of SiC rich layer [20,21]. The actual SiC concentration and the thickness of the produced layer depend on the conditions of the IBM and the initial layer structure. The mixing process of Si-C systems can be well described by TRIDYN simulation if the displacement

threshold energies are chosen to be the real Frenkel pair energies; this finding is verified by comparison of several experiments and simulations. The TRIDYN simulation provides depth profiles of the element but cannot tell anything about the compound formation. Based on experimental depth profiles measured by AES depth profiling we created a simple rule regarding the SiC compound formation: if concentration of C is lower than that of Si the whole amount of C converts to SiC and vice versa, but the amount of SiC cannot be larger than 80% (mole fraction). Therefore applying our simple rule the SiC concentration can be calculated from the results of the simulation [25]. Based on ref 25, for the present studies we have chosen such IBM (120 keV, $3x10^{16}$ Xe^{+} /cm^2 irradiation) and sample parameters (Si (20 nm) /C(10 nm) /Si (20 nm) /C (10 nm) multilayer structure) which result in relatively homogeneous 30-40 nm thick SiC rich layer. The multilayer structure was made by magnetron sputtering on Si single crystal substrate, and the ion irradiation was carried out by the Heavy Ion Cascade Implanter of the Institute for Particle and Nuclear Physics of the Wigner Research Centre for Physics in Budapest.

2.2. Production of patterned SiC

To demonstrate our procedure, two different patterns have been constructed, using Langmuir-Blodgett (LB) technique and usual lithography.

2.2.1. Langmuir-Blodgett technique + IBM

Silica nanospheres were deposited onto the sample applying Langmuir-Blodgett technique. Silica particles were synthesized by a seed-mediated method [26], which was slightly modified to fine-tune and achieve the appropriate diameter of the spheres. 192 μL diluted (10.000 fold) solution of silica seed particles (LUDOX AS-40, 40wt% in suspension, Sigma-Aldrich), 45 mL ethanol (99.97%, VWR International Ltd.), 1.17 mL ultrapure water and 7.05 mL NH_4OH solution (28-

30%, Reagent grade, Sigma-Aldrich) were mixed in a reaction vessel and stirred vigorously for 20 minutes. Silica precursor (tetraethyl orthosilicate, TEOS, 98%, Sigma-Aldrich) was added to the reaction mixture in 3 steps: 1.35 mL TEOS per 24 hours while the solution was stirred continuously. The diameter of the spheres was found to be 595 ± 9 nm measured by SEM. The excess of ammonia was removed by boiling until the pH of the sol reached the value of 7 (the evaporated EtOH was refilled continuously in order to presume preserve the initial concentration of the nanoparticles). The particles were centrifuged (3000 rcf, 5 minutes) and redispersed in EtOH:$CHCl_3$ mixture (1:2 volume ratio) and spread onto the air/water interface in a Wilhelmy film balance. After the compression and relaxation of the film, the monolayer was transferred to the substrate applying 7 mm/min withdrawal speed.

The LB film covered sample (Si (20 nm) /C (10 nm) /Si (20 nm) /C (10 nm)) was subjected to the chosen IBM (120 keV, $3x10^{16}$ Xe^+ /cm^2). The projected range of the 120 keV Xe^+ ions in SiO_2 is 58 nm [27], thus the SiO_2 covered part has not been affected by the ion bombardment. After the irradiation, the LB film was removed by lift-off using Scotch tape resulting in a chemical pattern made by irradiated (ion mixed) areas and not irradiated (Si) areas.

From this 2D pattern, a 3D structure can be made utilizing the different chemical entities on the surface; the etching and/or oxidation rates of the SiC rich region is strongly different from those of Si and C [22,25]. E.gs, by etching the sample in HF/HNO_3 solution for 10 min the pristine silicon layer is removed while the SiC rich region remains untouched resulting in a hole with a diameter determined by the arrangement of the SiO_2 spheres (typically 600 nm) and a depth of 20 nm. The bottom of the hole is made of C. Thus we will have a 3D structure made of C and SiC rich regions. This procedure might be followed by an oxidation process in microwave plasma during 10 minutes. This procedure removes the pristine carbon layer and leaves the SiC

rich region untouched, resulting in holes having a depth of 30 nm and the bottom consisting of Si (with native oxide cover), while the SiC rich region remain at the original place. If needed, this procedure could be repeated resulting in holes in SiC rich regions having various depths and either C or Si bottoms, that is, various 3D structures. For easier reference we will call these structures later as 3D patterned samples.

2.2.2. Lithographic technique +IBM

A grid of a periodicity of 2 μm served as a mask on the multilayer structure. The grid was a photoresist layer with a thickness of 1.3 μm which was transferred to the sample in a class 10-10000 clean room facility. After the irradiation the grid was removed by dipping the sample into fuming nitric acid and by oxidation in microwave plasma. The 3D structure was produced as above. For better visualization Figure 1. shows the whole process for producing the 3D structures.

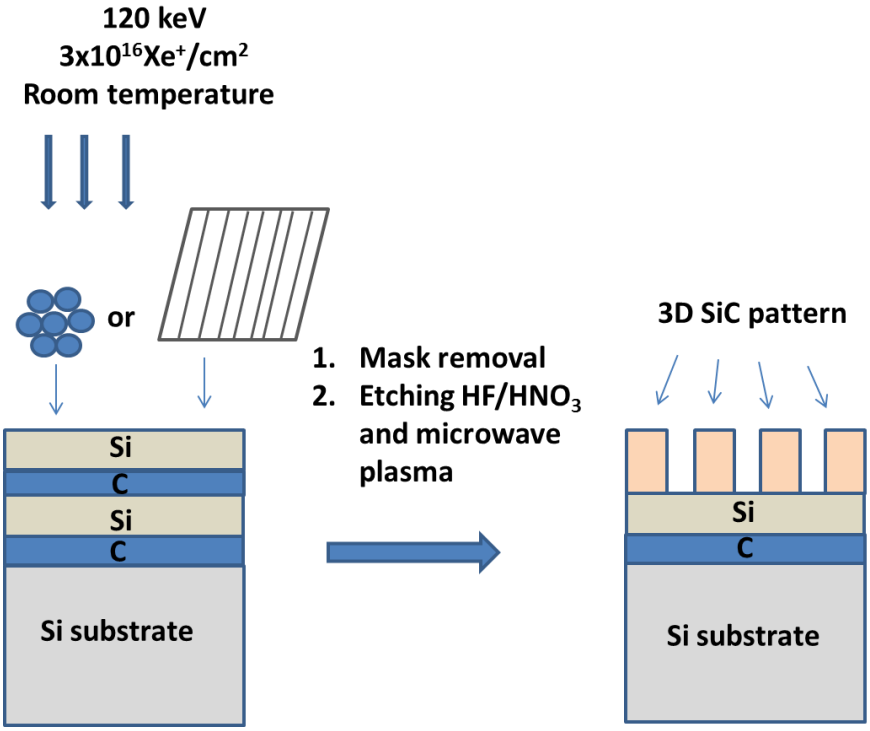

Figure 1. Process of producing 3D structures

2.3. AES depth profiling

AES depth profiling was applied to obtain the composition of the sample along the depth after various procedures. 1 keV Ar^+ ions were used for AES depth profiling with an angle of incidence of 80º with respect to the surface normal. To avoid heating effects a mild ion sputtering has been applied; the removal rate was about 0.2 nm/s. This was achieved by applying an ion beam current of about 4 $\mu A/mm^2$. The etch time was 20 s, ion etching area was diameter of about 500 μm. The ion current was kept constant during sputtering. The sample was rotated (6 rev/min) during ion bombardment. These parameters were selected to minimize the ion bombardment-induced surface and interface morphology changes [28]. The Auger spectra were recorded by a STAIB DESA 105 pre-retarded Cylindrical Mirror Analyzer (CMA) in direct current mode, the excitation energy was 5 keV.

The evaluation of the Auger spectra is described in detail elsewhere [20]. Its essential part is that the measured C (KLL) Auger peak is decomposed into graphitic and carbide components. Hence, the AES analysis gives four entities as C, Si, SiC and xenon and accordingly four in-depth distributions. We applied the relative sensitivity factor method for the calculation of the atomic concentrations [29].

2.4. Raman measurements

2.4.1. Sample preparation for microRaman measurements

LB patterned and etched (with or without Au coating) and non-patterned substrates were used in Raman measurements. The Au coating was made in an ATC ORION 8-E UHV e-beam evaporation system with an evaporation rate of 10 Å/s. In order to accumulate the reporter

molecules (Rhodamine 6G dye), 15 uL of $5 \cdot 10^{-5}$ M aqueous R6G solution was drop-casted onto the samples (~7x7 mm) and dried at room temperature.

2.4.2. MicroRaman spectroscopy

Raman spectra of R6G molecules were recorded by a single particle spectrometer. The optical setup consists of a dark-field upright microscope (Olympus BX-51) and a 100X objective (numerical aperture =0.9). The sample was placed onto an XYZ piezo stage (Physik Instrumente, P-545.3R8S) in order to position the area precisely for measurements. The illumination of the sample was achieved by an Ar laser (SpectraPhysics 165, λ = 514.5 nm) coupled to the microscope. The objective collected the scattered light, which was sent through a notch filter and a motorized slit prior to decomposition by a Princeton Instruments IsoPlane SCT-320 spectrometer. The spectrally decomposed light was detected by a cooled CCD camera (PIXIS 400 BRX). During the microRaman measurements, the integration time was set to 30 seconds and the laser power at the focal plane was 0.53 mW. The measured diameter of the laser spot illuminating the samples was 670 nm.

2.5. The determination of surface and/or geometrical patterning.

Surface morphologies of the patterned samples were also investigated by Scanning Electron Microscopy (SEM-LEO 1540 XB, operated at 5 keV) in SE mode and Atomic Force Microscopy (Bruker Multimode 8 AFM) in tapping mode.

3. RESULTS AND DISCUSSION

The masked multilayer samples have been irradiated by 120 keV, $3x10^{16}$ Xe^{+}/cm^{2} ions. Afterwards the mask was removed and we got the 2D structures where there are SiC rich regions

alongside pure Si. This 2D structure can be easily transformed with etching and oxidation steps to a well-defined 3D structure, namely to a 3D patterned sample. In this case the structure consists of SiC-rich regions at their original place and of holes of various depths with either carbon or Si at the bottom. Fig. 2a and b show SEM images of different magnifications – 20 kx and 50 kx, respectively - for the LB sample after mask removal and the etching procedure which consisted of HF/HNO_3 etching (removing a single Si layer) and oxidation in microwave plasma (removing a single C layer). As the SiC regions are resistant against these treatments, the SiC regions remain untouched only the regions not affected by ion bombardment will be altered. In the SEM image we can see strong contrast of whiter and darker regions. Since the contrast of the possible surface constituents - C, Si and SiC - are different, the SEM image is a draft visualization of the surface chemistry. In the present case (Fig. 2a and b) the surface consists of SiC rich regions (white) – where the irradiation took place - and Si regions (black), where the SiO_2 spheres shielded the sample and the first Si and the second C had been removed by the etching and oxidation procedures resulting in a hole of Si bottom. The structured surface shows a reasonably good homogeneity, and no major defects are observed. There are still dislocations in the hexagonal arrangements observed, likely due to polydispersities of the silica nanospheres as well as by the vertical lifting through the floating silica sphere monolayer. It is noteworthy to mention that the LB transfer is very effective and versatile as samples with large square centimeter surfaces can be fabricated with good quality [30]. Additionally, we can see lines between the places of the silica particles, this can be attributed to the neck formation between the particles due to ion beam induced sintering. This process is the result of the enormous surface tensions caused by the strong surface curvature at the contact points of nano-spheres. The surface tensions can be released by atom migration to the contact points of the spheres once surface

atoms get enough mobility due to the ion bombardment. As the mask deformations were observed to be of non-thermal nature and lead to necks between spheres reminiscent of a sintering process, the effect was called Ion Beam induced SIntering (IBSI) [31,32]. This means that the spaces between the particles have not been affected by the irradiation therefore the etching process attacked this area. The relative area (θ) of the irradiated region was calculated by applying the ImageJ program [33] and it was found to be 0.42. The AFM measurements of the 3D structure additionally provides the depth of the holes, (Fig. 2c) which proved to be of about 32 nm. This value agrees well with the expected one; this case we applied one step of HF/HNO_3 etching and one oxidation step, that is, we removed 20 nm Si and 10 nm C. The AFM images also show that the sides of the holes are reasonable straight.

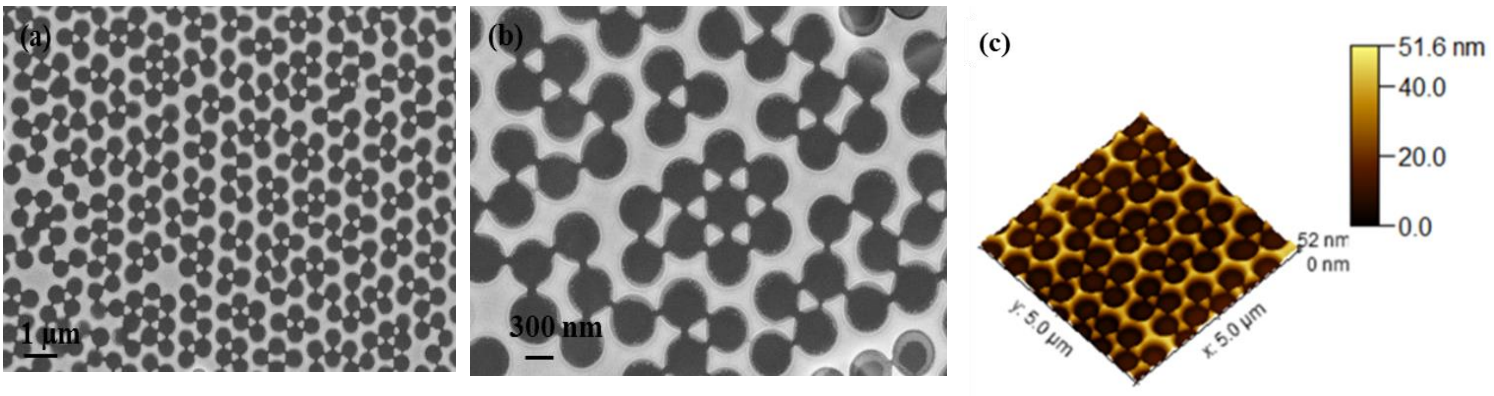

Fig. 2. a. b. SEM and c. AFM images of the LB-masked sample after mask removal and one step HF/HNO_3 etching and one step oxidation.

The micropatterns has been produced by applying lithographic grid as a mask is shown in Fig. 3. Fig. 3a and b show SEM images of different magnifications – 10 kx and 20 kx, respectively - after mask removal and HF/HNO_3 etching followed by oxidation and additional HF/HNO_3 etching. We can see that the structure became completely periodic and homogeneous. The relative area of the irradiated region was found to be 0.49. The depth of the etched holes is about

52 nm – as provided by AFM (Fig. 3c) – in good agreement with the expectation, since we have removed two Si layers amounting to 40 nm and one C layer of 10 nm – illustrating that a variety of hole depths can be achieved by varying the etching procedures.

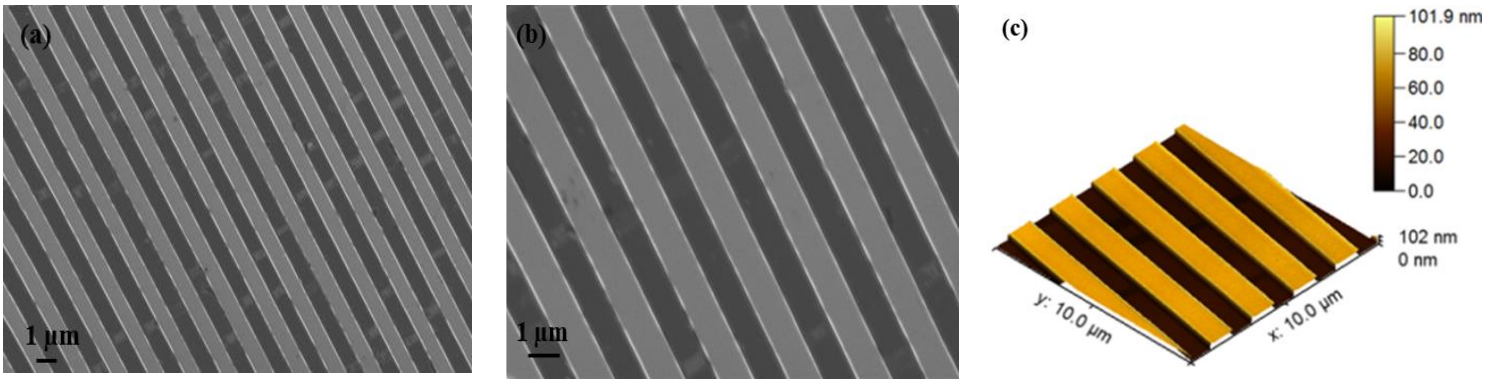

Fig. 3. a.b. SEM and c. AFM images of the grid-masked sample after mask removal and HF/HNO_3 etching, oxidation and additional HF/HNO_3 etching.

Though the SEM contrast gives important information on the geometrical arrangement of SiC rich regions, it obviously cannot describe the details of the actual surface concentration and in-depth concentration distribution of the SiC layer. However, these data are essential for determining the applicability of the sample. To get this information, AES depth profiling has been performed. The measured Auger spectrum was rather complex as the diameter of primary, exciting electron beam (50 µm) is much larger than the dimension of the patterning, thus the Auger spectrum measured on the patterned sample is a linear combination of Auger spectra emitted by the non-irradiated and irradiated parts of the sample. Moreover, the sputtering yields of the two distinct regions are different along the depth. Thus, the AES spectra emitted by the two regions originate from different depths. Since the sputtering yields of the different regions are known as well as the in-depth profile of the untouched region, we can calculate the AES spectrum emitted from the irradiated area from the measured AES spectrum as follows. The

measured in-depth profile is a series of concentration values belonging to various sputtering times. The in-depth profile of the untouched region is known from previous measurements and we can calculate the concentrations belonging to any sputtering time. We also know the relative area (determined from the SEM image by the help of the ImageJ code [33]) of the untouched region ($1-\theta$) and thus, the proportional part of the concentrations can be subtracted from the measured concentrations in all sputtering times. The result is the concentration belonging to the irradiated region after the given sputtering time, which can be compared with the Auger spectrum recorded from an unmasked similar sample after similar ion bombardment. Fig. 4. demonstrates the procedure in the case of the 2D structure; it shows the in-depth SiC profile (labeled as patterned irradiated) obtained from sample patterned by LB film and irradiated and after the LB film has been removed. The measured curve does not resemble the irradiated nor to the pristine sample. On the other hand, some of the elements, for example the sharp spikes resemble the features of the pristine samples, and the slowly varying concentrations resemble the irradiated one. Thus, we might hope that the combination of these two spectra results in the measured spectrum. As it is clear from Fig. 2 and previous discussion the regions under the SiO_2 spheres have not been reached by the irradiation thus they have the initial pristine structure; the corresponding in-depth profile (labeled as pristine) is also shown in Fig. 4. Thus, by subtracting $(1-\theta)$ times the SiC profile obtained from the pristine sample from the patterned-irradiated one leads to a curve (signed as calculated irradiated) which is the in-depth SiC profile of the irradiated region; it is a slowly varying SiC distribution. We can compare it with the θ times SiC in-depth profile obtained from sample which has not been patterned and was similarly irradiated (signed as non-patterned irradiated). The agreement is excellent. This means, that the patterning has not influenced the alteration at the irradiated region, which was in fact expected.

Consequently, in the irradiated area a quasi-homogeneous SiC rich layer formed. Thus, we could produce a patterned surface consisting SiC rich and Si regions in a well-defined geometrical structure.

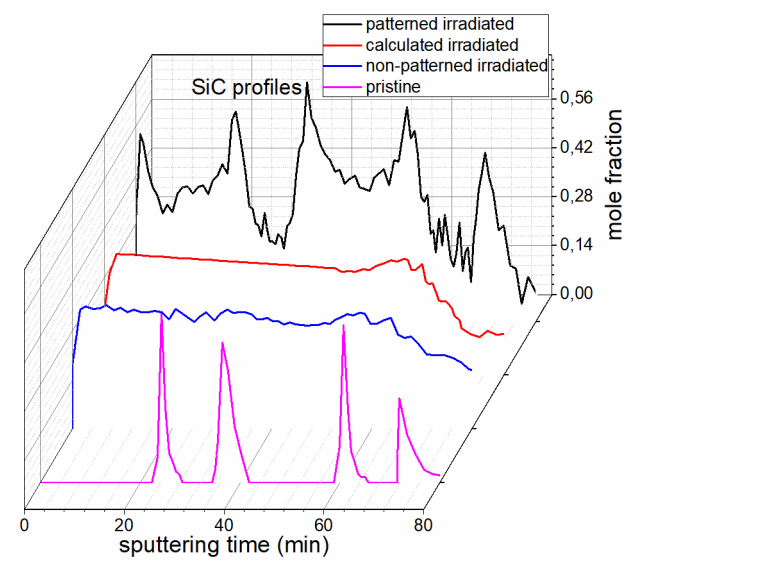

Fig. 4. SiC concentrations vs the sputtering time. The labels are as follows: patterned irradiated signs the curve measured on the irradiated patterned sample after removal of LB film; pristine curve is measured on pristine sample; calculated irradiated stands for curve calculated by substracting (1-θ) (determined from the SEM image) times the pristine curve from patterned irradiated; while non-patterned curve is measured on non-patterned sample irradiated similarly as the present one times θ.

To reveal a potential application of the patterned samples, Raman detection of an organic dye molecule (R6G) on the surface of the LB mask derived 3D structure was attempted. Raman spectroscopy is a non-contact and relatively easy, material characterization tool requiring no sample preparation. The Raman scattering process itself is weak but the surface-enhanced Raman scattering (SERS) technique allows the detection of low concentration of Raman active materials where the phenomenon occurs on roughened metallic surfaces. Mainly silver, copper and gold is used for these purposes. As gold is chemically and biologically inert we have applied it to check the Raman signal enhancement effect.

For this study we have used a sample which was irradiated through the LB mask, etched by HF/HNO_3 and oxidized to form a 3D structure (see Fig. 2) with a hole depth of 30 nm. The bottom of the hole was Si with thin oxide cover. In order to investigate the Raman scattering performance of this system, 10 nm gold was evaporated on its surface and also on the non-patterned irradiated one. The 3D patterned sample without gold coating was also examined for comparison purposes. The Raman activity was characterized by using reporter molecules of R6G. The Raman spectra were measured at 7 different locations over the sample location and averaged. The fluorescence background observed on the gold-coated samples was removed by applying Spectragryph program [34].

Fig. 5 shows typical Raman spectra obtained from the 3D patterned sample (curve a), non-patterned irradiated sample that is SiC-rich surface with gold coating (curve b) and the previous 3D patterned sample with gold coating (curve c); all surfaces were covered with R6G. We can see that the thin gold layer plays a crucial role in the surface enhancement of the Raman signal. In the case of 3D patterned sample without gold coating (curve a) only one intensive peak is visible at 520 cm^{-1} which corresponds to crystalline silicon; the well-defined Raman peaks of R6G cannot be observed. However, characteristic Raman signature of the reporter molecules can be obtained already on the gold coated non-patterned samples (curve b). The spectra exhibit strong lines at 611, 773, 1127, 1183, 1310, 1360, 1507, 1573, and 1648 cm^{-1}; these peak positions agree well with the ones measured on pure Ag [35] and Au [36]. A further 3-fold increase of the characteristic SERS signals of R6G was observed on the surface of the gold-coated 3D patterned sample.

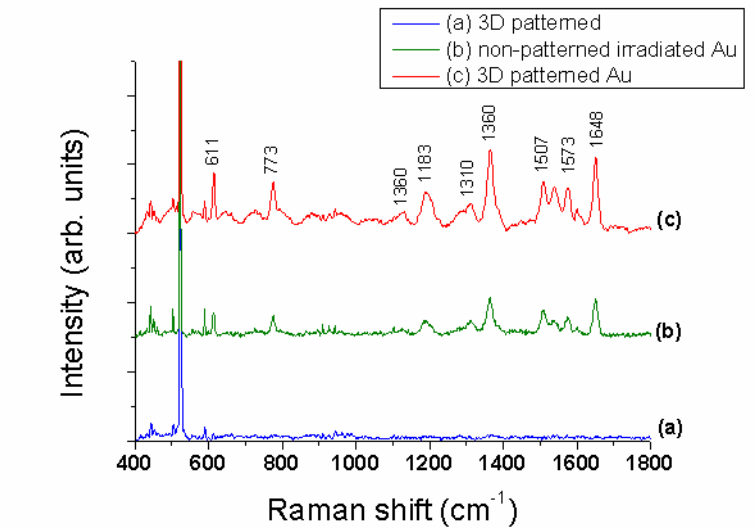

Fig. 5. Raman spectra of rhodamine 6G after background removal on different surfaces: (a) 3D patterned surface, which means irradiated through LB mask and etched (b) Au evaporated non-patterned irradiated surface (c) Au evaporated 3D patterned surface. The R6G concentration was 5 x 10^{-5} M, the excitation wavelength 514.5 nm.

Fig. 6. shows AFM images obtained from the gold coated non-patterned and gold coated 3D patterned samples. It is clear that the two surfaces are strongly different. The roughness parameter, R_a, could be extracted from the measurements to be 1.8 nm and 11.2 nm, respectively.

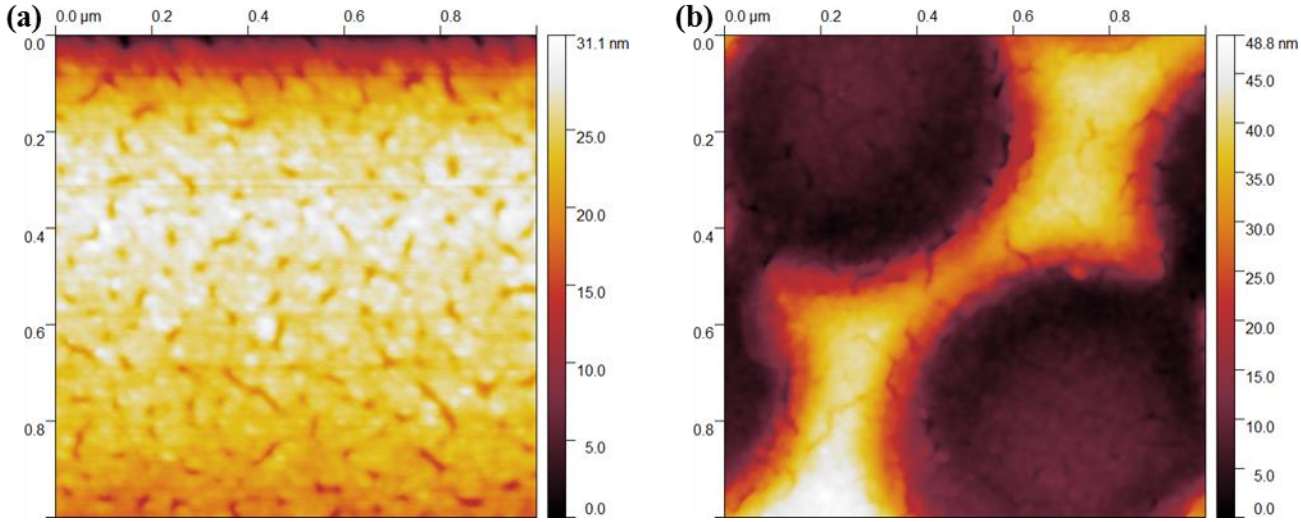

R_a = 1.8 nm R_a = 11.2 nm

Fig. 6. AFM images of the a. gold coated non-patterned and b. gold coated 3D patterned samples

The patterned surface possesses approximately 6-fold higher roughness than the non-patterned one. Therefore the increased SERS signal on the gold coated 3D patterned surface may be attributed to the increased roughness of the structured surface as a result of 3D patterning. This is in good agreement with the general expectation that increasing roughness can be a powerful tool to increase the Raman scattering effect [37-40]. The surface enhanced Raman peaks of the R6G on our gold-coated 3D patterned samples, which contains SiC, C having high resistance against chemical attacks offers the possibility for high sensitivity sensors operating in harsh environment and due to the biocompatibility of SiC for detection of biomolecules, as well.

4. CONCLUSIONS

A novel method has been demonstrated to produce SiC patterns at room temperature which is scalable up to wafer size. Two differently masked (LB film and lithographic grid) Si (20 nm)/C (10 nm)/ Si (20 nm)/ C (10 nm) /Si substrates have been irradiated by 120 keV, $3x10^{16}$ Xe^{+}/cm^{2}. Due to IBM a SiC rich layer formation on the non-covered parts of the sample was demonstrated using AES depth-profiling, while the covered regions have not changed. Thus, in a single-step (the compound formation and the creation of patterns happened in one step) a tailor made 2D nanopattern of SiC rich regions alongside pure Si has been constructed at room temperature. Applying additional etching and oxidation processes the 2D pattern has been transformed to a 3D one consisting SiC rich regions in their original place and holes of given depths with either C or Si bottom. The gold coated 3D structure proved to be SERS active allowing the high sensitivity detection of biomolecules both in mild and harsh environments.

AUTHOR INFORMATION

Corresponding Author

*E-mail: menyhard.miklos@energia.mta.hu

ACKNOWLEDGEMENT

The work was supported by Pro Progressio Foundation. Thanks for M. Eros for the grid lithography and for D. K. Menyhard for useful remarks.

REFERENCES

[1] J. Mukherjee, S. Ghosh, A. Ghosh, Enhanced nano-mechanical and wear properties of polycarbosilane derived SiC coating on silicon, Appl. Surf. Sci. 325 (2015) 39–44.

[2] R. Maboudian, C. Carraro, D.G. Senesky, C.S. Roper, Advances in silicon carbide science and technology at the micro- and nanoscales, J. Vac. Sci. Technol. A 31 (2013) 50805–50818.

[3] M. Frischmuth, Schneider, D. Maurer, T. Grille, U.T. Schmid, Inductively-coupled plasma-enhanced chemical vapour deposition of hydrogenated amorphous silicon carbide thin films for MEMS, Sens. Actuators A 247 (2016) 647–655.

[4] M. Sarro, Silicon carbide as a new MEMS technology, Sens. and Act. 82 (2000) 210-218.

[5] R. Cheung, Silicon Carbide Micro Electromechanical Systems for Harsh Environments, first ed.; Imperial College Press, 2006.

[6] C.A. Zorman, M. Mehregany, SiC MEMS: opportunities and challenges for applications in harsh environments, Thin Solid Films 355 (1999) 518-524.

[7] T. Tsvetkova, S. Takahashi, A. Zayats, P. Dawson, R. Turner, L. Bischoff, O. Angelov, D. Dimova-Malinovska, Fabrication of nano-scale optical patterns in amorphous silicon carbide with focused ion beam writing, Vacuum 79 (2005) 100–105.

[8] C.A. Zorman, R.J Parro, Micro- and nanomechanical structures for silicon carbide MEMS and NEMS, Phys. Stat. Sol. B 254 (2008) 245 1404–1424.

[9] E.A. Filatova, D. Hausmann, S.D. Elliott, Understanding the Mechanism of SiC Plasma-Enhanced Chemical Vapor Deposition (PECVD) and Developing Routes toward SiC Atomic Layer Deposition (ALD) with Density Functional Theory, ACS Appl. Mater. Interfaces 10 (2018) 15216−15225.

[10] W. Zhou, J. Wang, J. Zhang, X. Li, G. Min, Large area fabrication of 3D petal-like nanopattern for surface enhanced Raman scattering, Appl. Surf. Sci. 303 (2014) 84– 89.

[11] L. Pramatarova, E. Pecheva, M.F. Maitz, M.T. Pham, A. Kondyurin, Ion beam patterning of solid surfaces for hydroxyapatite deposition, Vacuum 76 (2004) 335-338.

[12] J. Szivos, M. Serenyi, E. Gergely-Fulop, T. Lohner, G. Safran, Nanopattern formation in UV laser treated a-AlOx and nc-Al/AlOx layers, Vacuum 109 (2014) 200-205.

[13] G.H.Takaoka, H. Ryuto, R. Ozaki, H. Mukai, M. Takeuchi, Micro-patterning of Si(100) surfaces by ethanol cluster ion beams, Surf. Coat. Technol. 206 (2011) 869-873.

[14] X. Jia, T. Q. Jia, L.E. Ding, P.X. Xiong, L. Deng, Z.R. Sun, Z. G. Wang, J.R. Qiu, Z.Z. Xu, Complex periodic micro/nanostructures on 6H-SiC crystal induced by the interference of three femtosecond laser beams, Opt. Lett. 34 (2009) 788–790.

[15] D. G. Merkel, L. Bottyan, F. Tancziko, Z. Zolnai, N. Nagy, G. Vertesy, J. Waizinger, L. Bommer, Magnetic patterning perpendicular anisotropy FePd alloy films by masked ion irradiation, J. Appl.Phys. 109 (2011) 124302-124309.

[16] A. L. Stepanov, F. Galyautdinov, A. B. Evlyukhin, V. I. Nuzhdin, V. F. Valeev, Y. N. Osin, E. A. Evlyukhin, R. Kiyan, T. S. Kavetskyy, B. N. Chichkov, Synthesis of periodic

plasmonicmicrostructures with copper nanoparticlesin silica glass by low-energy ion implantation, Appl. Phys. A 111 (2012) 261-264.

[17] W. Guan, I. M. Ross, U. M. Bhatt, J. Ghatak, N. Peng, B J. Inkson, G. Möbus, Nanopatterning by ion implantation through nanoporous alumina masks, Phys. Chem. Chem. Phys. 15 (2013) 4291-4296.

[18] E. Albert, P. Basa, A. Deák, A. Németh, Z. Osváth, G. Sáfrán, Z. Zolnai, Z. Hórvölgyi, N. Nagy, Introducing nanoscaled surface morphology and percolation barrier network into mesoporous silica coatings, RSC Adv. 5 (2015) 60041-60053.

[19] Sigmund, P.; Gras-Marti, Theoretical aspects of atomic mixing by ion beams, Nucl. Instrum Methods Phys. Res. B 182/183 (1981) 25-41.

[20] A. Barna, S. Gurban, L. Kotis, J. Labar, A. Sulyok, A.L. Toth, M. Menyhard, J. Kovac, P. Panjan, Growth of amorphous SiC film on Si by means of ion beam induced mixing, Appl. Surf. Sci. 263 (2012) 367–372.

[21] G. Battistig, S. Gurban, G. Safran, A. Sulyok, A. Németh, P. Panjan, Z. Zolnai, M. Menyhard, Wafer-scale SiC rich nano-coating layer by Ar^+ and Xe^+ ion mixing, Surf. Coat. Technol. 302 (2016) 320–326.

[22] A.S. Racz, Z. Kerner, A.Nemeth, P. Panjan, L. Peter, A.Sulyok, G. Vertesy, Z. Zolnai, M Menyhard, Corrosion resistance of nano-sized SiC rich composite coatings produced by noble gas ion mixing, ACS Appl. Mater. Interfaces 9 (2017) 44892–44899.

[23] M.K. Kuntumalla, V.V.S.S. Srikanth, S. Ravulapalli, U. Gangadharini, H. Ojha, N.R. Desai, C. Bansal, SERS activity of Ag decorated nanodiamond and nano-b-SiC, diamond-like-carbon and thermally annealed diamond thin film surfaces, Phys. Chem. Chem. Phys. 17 (2015) 21331.

[24] X.S. Zhang, B. Meng, F.Y. Zhu, W. Tang, H.X. Zhang, Switchable wetting and flexible SiC thin film with nanostructures for microfluidic surface-enhanced Raman scattering sensors, Sens. and Act. A 208 (2014) 166– 173.

[25] A.S. Racz, M. Menyhard, Design of corrosion resistive SiC nano-layers. ACS Appl. Mater. Interfaces 10 (2018) 22851–22856.

[26] S.L. Chen, G. Yuan, C.T. Hu, Preparation and Size Determination of Monodisperse Silica Microspheres for Particle Size Certified Reference Materials, Powder Technol. 207 (2011) 232–237.

[27] SRIM Stopping and range of ions in matter by J.F. Ziegler, version SRIM, 2013 Software freely available www.srim.org

[28] M. Menyhard, High-depth-resolution Auger depth profiling/atomic mixing, Micron 30 (1999) 255–265.

[29] K.D. Childs, B.A. Carlson, L.A. LaVanier, J.F. Moulder, D.F. Paul, W.F. Stickle, (Eds.), Handbook of Auger Electron Spectroscopy, 3rd ed.; D.G. Watson Eden Prairie, Minnesota, 1995.

[30] N. Marquestaut, A. Martin, D. Talaga, L. Servant, S. Ravaine, S. Reculusa, D.M. Bassani, E. Gillies, F. Lagugné-Labarthet, Raman Enhancement of Azobenzene Monolayers on Substrates Prepared by Langmuir-Blodgett Deposition and Electron-Beam Lithography Techniques, Langmuir 24 (2008) 11313-11321.

[31] D. Kraus, J.K.N. Lindner, B. Stritzker, Ion beam induced sintering of colloidal polystyrene nano-masks, Nucl. Instrum. Methods Phys. Res. B 257 (2007) 455–458.

[32] N. Nagy, Z. Zolnai, E. Fülöp, A. Deák, I. Bársony, Tunable ion-swelling for nanopatterning of macroscopic surfaces: The role of proximity effects Appl. Surf. Sci. 259 (2012) 331– 337.

[33] M.D. Abramoff, P.J. Magalhaes, S.J. Ram, Image Processing with ImageJ. J. Biophotonics 11 (2004) 36-42.

[34] Spectragryph-optical spectroscopy software by F. Menges, version 1.2.9, 2018 Software freely available www.effemm2.de/spectragryph

[35] J. Rahomaki, T. Nuutinen, L. Karvonen, S. Honkanen, P. Vahimaa, Horizontal Slot Waveguide Channel for Enhanced Raman Scattering. Opt. Express 21 (2013) 9060-9068.

[36] L.B. Luo, L.M. Chen, M.L. Zhang, Z.B. He, W.F. Zhang, G.D. Yuan, W.J. Zhang, S.T. Lee, Surface-Enhanced Raman Scattering from Uniform Gold and Silver Nanoparticle-Coated Substrates, J. Phys. Chem. C 113 (2009) 113 9191–9196.

[37] C. Lee, C.S. Robertson, A.H. Nguyen, M. Kahraman, S. Wachsmann-Hogiu, Thickness of a metallic film, in addition to its roughness, plays a significant role in SERS activity, Sci. Rep. 5 (2015) 5 11644-11652.

[38] M. Yang, Q. Wu, J. Qi, I. Drevensek-Olenik, Z. Chen, Y. Pan, J. Xu, Microstructured polymer-based substrates with broadband absorption for surface enhanced Raman scattering, J. Raman Spectrosc. 44 (2013) 1678–1681.

[39] O. Prakash, P. Gautam, S. Kumar, P. Singh, R.K. Dani, M.K. Bharty, N.K. Singh, A.K. Ghosh, V. Deckert, R.K. Singh, Surface enhanced Raman scattering investigation of two novel piperazine carbodithioic acids adsorbed on Ag and ZnO nanoparticles, RSC Adv. 5 (2015) 5571-5579.

[40] S. Basuray, A. Pathak, S. Bok, B. Chen, S.C. Hamm, C.J. Mathai, S. Guha, K. Gangopadhyay, S. Gangopadhyay, Plasmonic nano-protrusions: hierarchical nanostructures for single-molecule Raman spectroscopy, Nanotechnology 28 (2017) 28 025302-025314.

Graphical abstract: